

**Kinetically "Locked" Metallomacrocycle**

Journal:	<i>Dalton Transactions</i>
Manuscript ID	DT-ART-11-2015-004635.R1
Article Type:	Paper
Date Submitted by the Author:	05-Jan-2016
Complete List of Authors:	Nishino, Toshio; Nagoya University, Department of Chemistry, Graduate School of Science Yamada, Yasuyuki; Nagoya University, Department of Chemistry, Graduate School of Science; Nagoya University, Research Center for Materials Science Akine, Shigehisa; Kanazawa University, Graduate School of Natural Science and Technology Sugimoto, Kunihisa; Japan Synchrotron Radiation Research Institute, Research and Utilization Division Tanaka, Kentaro; Nagoya University, Department of Chemistry, Graduate School of Science



Journal Name

ARTICLE

Kinetically “Locked” Metallomacrocycle

Toshio Nishino,^a Yasuyuki Yamada,^{a,b} Shigehisa Akine,^c Kuniyoshi Sugimoto^d and Kentaro Tanaka*^a

Received 00th January 20xx,
Accepted 00th January 20xx

DOI: 10.1039/x0xx00000x

www.rsc.org/

Self-assembly based on reversible metal–ligand bond formation is useful for the synthesis of discrete supramolecular nanoarchitectures. However, the architectures constructed by this technique sometimes suffer from kinetic instability due to the dissociation of metal–ligand bonds, especially under highly diluted conditions or in the presence of competitive ligands or metal ions. In this study, a kinetically stabilized metallomacrocycle was synthesized in one pot via the combination of metal-mediated self-assembly and subsequent oxidative “locking” of the coordination bonds. The macrocycle consists of four Co ions and four bis-bidentate ligands L^{2-} . The complexation of labile Co(II) ions with the ligands afforded the macrocycle with four-fold rotational symmetry, exhibiting the right-angled geometries of the β -diketonate ligands on the carbazole. The subsequent oxidation of the Co(II) ions inside the macrocycle into Co(III) ions made the metal–ligand bonds almost inert, thus affording a kinetically locked 4:4 metallomacrocycle. This macrocycle showed high stability even in the presence of an excess amount of competitive ligands. The X-ray crystallography of the macrocycle indicated that it assembled in a columnar manner, forming one-dimensional nanochannels in the middle of the column.

Introduction

The development of methods to synthesize discrete and robust nanoarchitectures is indispensable to expand bottom-up nanotechnologies. Metal-mediated self-assemblies are powerful processes for the spontaneous synthesis of nanoarchitectures from appropriately designed ligands as the small building blocks and metal ions as the multidirectional connectors.¹ The self-assembly process requires fast and reversible metal–ligand bond formation. Because the polyfunctional precursors have possibility to afford many reaction products before the reaction reaches the most thermodynamically stable compound, the association/dissociation of the metal–ligand bonds is essential to repair the structures. For the past several decades, this approach has been widely used to synthesize various discrete molecular architectures such as molecular cages,² molecular nanotubes,³ and metallomacrocycles.⁴ For example, Fujita quantitatively synthesized a discrete molecular square by the metal complexation of 4,4'-bipyridine with a Pd complex in his pioneering work.^{4a} He has recently expanded the approach to construct a spherical giant molecular cage with a periphery

diameter of ~5 nm via the bond formation among the pyridine moieties and Pd ions.⁵

On the other hand, the reversible bond formation in self-assembly processes causes the deformation of nanostructures in highly diluted solutions, and exchange reactions occur in the presence of other metal ions or ligands. To solve this problem between the self-assembly process and structural instability, it is promising to use synthetic strategies that involve two successive steps, metal-mediated self-assembly and “locking” the metal–ligand bonds after the construction of the thermodynamically stable species. For example, Fujita synthesized a robust and stable nanocage composed of kinetically inert Pt(II)–pyridine bonds that were sufficiently labilized to rearrange the bonds only in a solution of 2,2,2-trifluoroethanol.⁶ As another example, Sauvage⁷ and Leigh⁸ independently demonstrated efficient post-synthesis covalent bond formation to “lock” the structure of the self-assembled metal complexes. The other practical method for this purpose is to change the characteristics of the metal centers by oxidation after the self-assembly. Metal ions with higher oxidation states form kinetically stable coordination bonds than those with lower oxidation states. For example, Co(II) ion is sufficiently labile for the self-assembly approaches, whereas Co(III) ion is sufficiently inert to lock the structure. For example, the metal–ligand exchange rate of $\text{Co(II)(H}_2\text{O)}_6$ in an aqueous solution is $3 \times 10^6 \text{ s}^{-1}$; however, it is $<10^{-6} \text{ s}^{-1}$ for $\text{Co(III)(H}_2\text{O)}_6$.⁹ Recently, many pioneering studies have been reported. Williams and Pigué et al. synthesized triple helical dinuclear Co(III) complexes¹⁰ via this strategy. Kinetically inert Cr(III) helicates were also synthesized in a similar manner.¹¹ Lusby *et al.* quantitatively synthesized a kinetically locked tetrahedral

^a Department of Chemistry, Faculty of Science, Nagoya University, Furo-cho, Chikusa-ku, Nagoya, 464-8602, Japan. E-mail: kentaro@chem.nagoya-u.ac.jp

^b Research Center for Materials Science, Nagoya University, Furo-cho, Chikusa-ku, Nagoya, 464-8602, Japan.

^c Graduate School of Natural Science and Technology, Kanazawa University, Kakuma-machi, Kanazawa, 920-1192, Japan.

^d Japan Synchrotron Radiation Research Institute, 1-1-1, Kouto, Sayo-cho, Sayo-gun, Hyogo, 679-5198, Japan

† Electronic Supplementary Information (ESI) available. See DOI: 10.1039/x0xx00000x

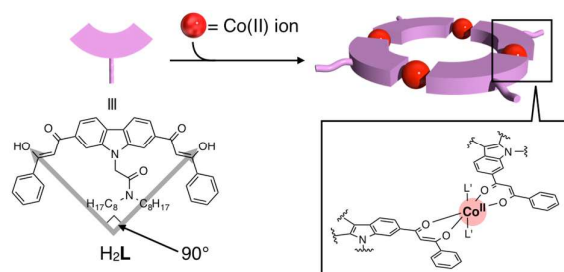


Figure 1. Formation of macrocycle by self-assembly between H_2L and $Co(II)$ ion.

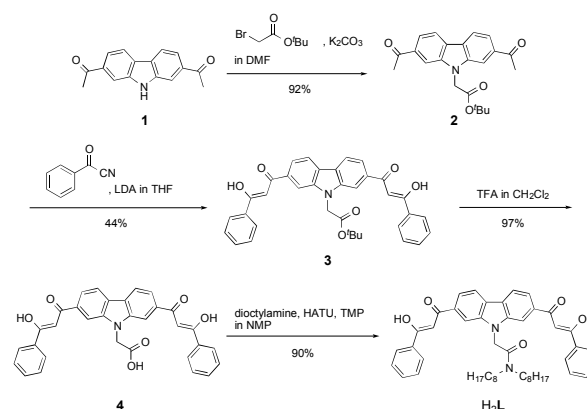
molecular cage composed of six bridging ligands and four $Co(III)$ ions.¹²

Here, we report the synthesis of a square-shaped metallomacrocycle with a “locked” structure via the complexation of $Co(II)$ ions with a metal ligand bearing two β -diketones, followed by the oxidation of the $Co(II)$ centers to $Co(III)$. We designed a carbazole bearing two β -diketones at the 2 and 7 positions. Because β -diketones form neutral ML_2 complexes with meridional coordination geometries (either *cis*- or *trans*- configuration) with $Co(II)$ ion, we expected that carbazole H_2L bearing two β -diketones forms a square-shaped 4:4 metallomacrocycle with $Co(II)$ ions by self-assembly, exhibiting the right-angled geometries of the β -diketonate ligands on the carbazole as shown in Figure 1. Because H_2L has a rigid structure and the metal–ligand exchange rate between β -diketones and $Co(II)$ ions is high, we assumed that the macrocycle would be the thermodynamically stable product compared to the corresponding polymeric species.

Result and discussion

Synthesis of Ligand H_2L .

The synthesis of carbazole, H_2L , is shown in Scheme 1. The nitrogen of 2,7-diacetyl-9H-carbazole **1**¹³ was alkylated with *t*-butyl bromoacetate, affording compound **2**.¹⁴ The acetyl groups were converted to β -diketones via the generation of ketoenolates using lithium diisopropylamide followed by Claisen condensation with benzoyl cyanide¹⁵ in 44% yield. After the *t*-butyl group of compound **3** was removed using trifluoroacetic acid, dioctylamine was condensed with the acetate to increase the solubility.



Scheme 1. Synthesis of carbazole H_2L bearing two β -diketones.

Self-Assembly of 4:4 Macrocycle by $Co(II)$ complexation.

The complexation behavior of the ligand H_2L (10 μM) with $Co(II)$ ion was investigated by UV–visible titration. The metal-free ligand H_2L has an absorption maximum at 390 nm in $CHCl_3$ in the presence of 2 equiv of base, 1,8-diazabicyclo[5.4.0]undec-7-ene (DBU), as represented by the solid curve in Figure 2. Upon each addition of $Co(OAc)_2$, the complexation equilibrated immediately (Figure S1). The absorption at 390 nm linearly decreased with clear isosbestic points at 357 nm and 424 nm until 1 equiv of $Co(II)$ ion was added. This indicates that L^{2-} coordinated to $Co(II)$ ion in a 1:1 ratio. Moreover, the matrix-assisted laser desorption/ionization time-of-flight mass spectrometry (MALDI-TOF MS) spectrum of the mixture containing H_2L (10 μM), $Co(OAc)_2$ (1 equiv), and DBU (2 equiv) showed the peaks corresponding to a 4:4 macrocyclic complex at $m/z = 3191$ (Figure 3). The species bearing axial ligands were not observed under this MS condition. We assumed that the peaks at m/z 2394 (corresponding to the $Co(II)_3L_3$), m/z 2337 (corresponding to the $Co(II)_2L_3$), m/z 1597 (corresponding to the $Co(II)_2L_2$), and m/z 1539 (corresponding to the $Co(II)L_2$) in the MALDI MS spectrum were generated during the ionization process as often observed in the case of metallosupramolecules. These results indicate that the desired 4:4 macrocyclic complex was formed preferentially when an equimolar amount of H_2L and $Co(II)$ ion was used. The K_a value for the 1:1 complexation of the bis(β -diketone) ligand H_2L with $Co(II)$ ions was estimated to be $>10^5 M^{-1}$, comparable to the K_a value ($10^{5.77} M^{-1}$ in 1,4-dioxane/ $H_2O = 1:1$) of the 1:1 complexation of acetylacetone,¹⁶ a typical β -diketone ligand, with $Co(II)$ ion.

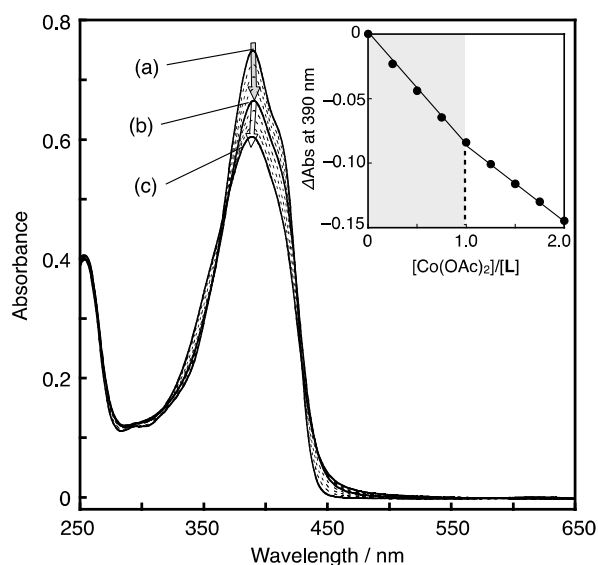


Figure 2. UV-visible absorption spectral change of H_2L ($10 \mu\text{M}$) upon the addition of $\text{Co}(\text{OAc})_2$ in the presence of $20 \mu\text{M}$ of DBU in CHCl_3 at 20°C . UV-visible spectra of H_2L (a) before the addition of $\text{Co}(\text{II})$ ion, (b) after the addition of $10 \mu\text{M}$ (1 equiv of H_2L) of $\text{Co}(\text{OAc})_2$, and (c) after the addition of $20 \mu\text{M}$ (2 equiv of H_2L) of $\text{Co}(\text{OAc})_2$. The inset shows the change in the absorption at 390 nm upon the addition of $\text{Co}(\text{II})$ ion against H_2L .

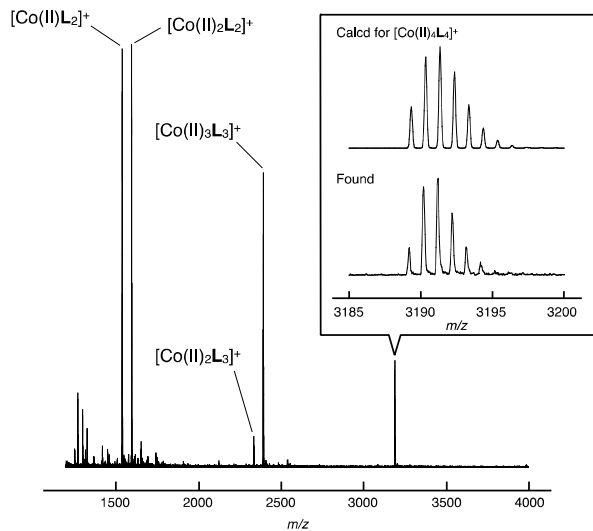
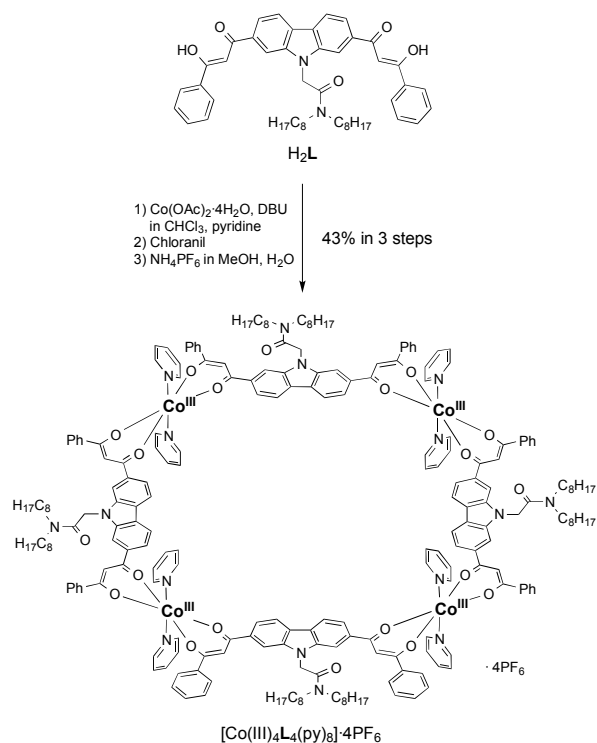


Figure 3. MALDI-TOF MS spectrum of a CHCl_3 solution containing H_2L ($10 \mu\text{M}$), $\text{Co}(\text{OAc})_2$ ($10 \mu\text{M}$), and DBU ($20 \mu\text{M}$). The inset shows the comparison of an expansion of the spectrum with the calculated isotope distribution pattern for the corresponding charge of the molecular ion.

The addition of >1 equiv of $\text{Co}(\text{II})$ ion caused deviation from the consistent spectral change, and the absorption decreased at 390 nm and increased at 350 nm . This indicates that the 4:4 macrocycle is kinetically unstable and decomposed in the presence of an excess amount of $\text{Co}(\text{II})$ ion. Although we attempted to isolate this macrocycle by silica gel column chromatography or gel permeation chromatography, we could not isolate it because it decomposed during the purification due to its kinetic instability.

“Locking” the Structure of Macrocycle.

The macrocyclic structure can be “locked” and isolated after oxidizing the $\text{Co}(\text{II})$ centers to $\text{Co}(\text{III})$ s. $\text{Co}(\text{II})_4\text{L}_4(\text{py})_8$ was synthesized by the condensation of 1 mM H_2L with $\text{Co}(\text{OAc})_2$ in the presence of DBU in CHCl_3 containing an excess amount of pyridine (62 mM); then, the generated macrocycle was oxidized with chloranil, affording the structurally “locked” tetracationic macrocycle $[\text{Co}(\text{III})_4\text{L}_4(\text{py})_8]\cdot 4\text{PF}_6$, where the two pyridines coordinated to each of the four $\text{Co}(\text{III})$ centers at the axial positions, in 43% isolated yield (Scheme 2).¹⁷ The macrocycle $[\text{Co}(\text{III})_4\text{L}_4(\text{py})_8]\cdot 4\text{PF}_6$ was purified by silica gel column chromatography unlike the macrocycle with $\text{Co}(\text{II})$ centers. This clearly indicates the higher kinetic stability and robustness of $[\text{Co}(\text{III})_4\text{L}_4(\text{py})_8]\cdot 4\text{PF}_6$ than $\text{Co}(\text{II})_4\text{L}_4(\text{py})_8$. The structure of $[\text{Co}(\text{III})_4\text{L}_4(\text{py})_8]\cdot 4\text{PF}_6$ was fully characterized by ^1H -NMR, COSY, and ESI-TOF MS spectroscopies and single-crystal X-ray structural analysis.



Scheme 2. Synthesis of **L**: $\text{Co}(\text{III})$ ion = 4:4 macrocycle $[\text{Co}(\text{III})_4\text{L}_4(\text{py})_8] \cdot 4\text{PF}_6$.

The ESI-TOF MS data showed the molecular ion peaks at m/z 2056.8 ($z = 2$), 1322.9 ($z = 3$), and 955.9 ($z = 4$), confirming the structure of the desired macrocycle $[\text{Co}(\text{III})_4\text{L}_4(\text{py})_8] \cdot 4\text{PF}_6$ (Figure 4). Figure 5 shows the comparison of the aromatic region of the $^1\text{H-NMR}$ spectrum of ligand H_2L (Figure 5(a)) with that of $[\text{Co}(\text{III})_4\text{L}_4(\text{py})_8] \cdot 4\text{PF}_6$ (Figure 5(b)) in CDCl_3 . As shown in Figure 5(b) (for the full $^1\text{H-NMR}$ spectrum, see Figure S2), all the narrow signals in the $^1\text{H-NMR}$ spectrum of $[\text{Co}(\text{III})_4\text{L}_4(\text{py})_8] \cdot 4\text{PF}_6$ could be assigned to one-quarter of the entire structure of $[\text{Co}(\text{III})_4\text{L}_4(\text{py})_8] \cdot 4\text{PF}_6$, indicating that the macrocycle has a diamagnetic character owing to the low-spin octahedral $\text{Co}(\text{III})$ centers with a C_4 symmetrical structure in the solution. The signal corresponding to the enolic proton of H_2L at δ 17.06 ppm disappeared after the complexation with $\text{Co}(\text{III})$ ion. Moreover, almost all the aromatic protons of the carbazole of $[\text{Co}(\text{III})_4\text{L}_4(\text{py})_8] \cdot 4\text{PF}_6$ showed significant downfield shifts compared to those of H_2L . The protons of axial pyridines also showed downfield shifts (Figure S3). These shifts can be attributed to the decrease in the electron densities of these ligands upon metal coordination and the shielding from the neighboring ligands. In comparison, the signals of the methine protons of β -diketone and the 1- and 8-positions of the carbazole of $[\text{Co}(\text{III})_4\text{L}_4(\text{py})_8] \cdot 4\text{PF}_6$ showed upfield shifts. Moreover, only these protons showed significant upfield shifts with the counteranions of $[\text{Co}(\text{III})_4\text{L}_4(\text{py})_8]^{4+}$ (Figure S4 and Table S1) compared to the slight signal shifts of the other protons. Therefore, the counteranions preferentially reside in the proximity of these protons in a solution.

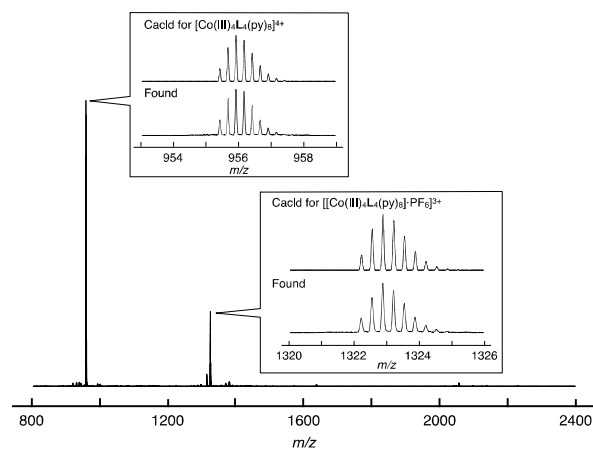


Figure 4. ESI-TOF MS spectrum of the macrocycle $[\text{Co}(\text{III})_4\text{L}_4(\text{py})_8] \cdot 4\text{PF}_6$. The inset shows the comparison of an expansion of the measured spectra with the calculated isotope distribution pattern for the corresponding charge of the molecular ion.

The crystals of $[\text{Co}(\text{III})_4\text{L}_4(\text{py})_8] \cdot 4\text{PF}_6$ suitable for X-ray structural analysis were obtained by the slow evaporation of a 1:1 solution of CH_2Cl_2 and toluene. The use of synchrotron radiation confirmed the structure of $[\text{Co}(\text{III})_4\text{L}_4(\text{py})_8] \cdot 4\text{PF}_6$. As shown in Figure 6(a), the macrocycle has a square structure, comprising four L^{2-} ligands, four $\text{Co}(\text{III})$ ions, and two pyridines coordinated to each Co center from the above and below. The size of the inner cavity of the macrocycle was approximately $11 \times 11 \text{ \AA}^2$. PF_6^- anions and CH_2Cl_2 molecules, the counteranions of the $\text{Co}(\text{III})$ centers and crystal solvent respectively, reside inside the cavity, whereas the other PF_6^- anions reside outside (see Figure 6(a)). $[\text{Co}(\text{III})_4\text{L}_4(\text{py})_8] \cdot 4\text{PF}_6$ macrocycle has an almost planar structure. In the packing structure of the crystal, the macrocycle forms an offset column by slipped stacking with a spacing of 7.8 \AA (Figure 6(b)); thus, a nanochannel was generated along the a -axis containing PF_6^- , CH_2Cl_2 , and parts of alkyl side chains (Figure 6(c)).

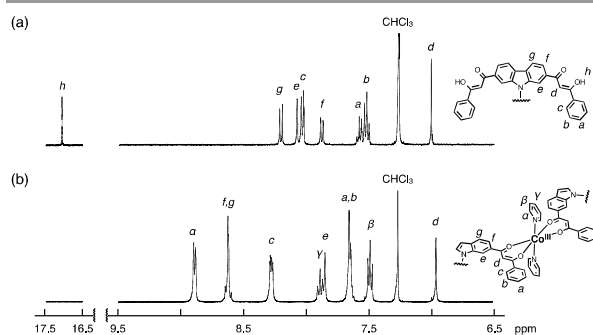


Figure 5. Aromatic region of the $^1\text{H-NMR}$ spectrum of (a) H_2L and (b) $[\text{Co}(\text{III})_4\text{L}_4(\text{py})_8] \cdot 4\text{PF}_6$ (400 MHz, CDCl_3/TMS).

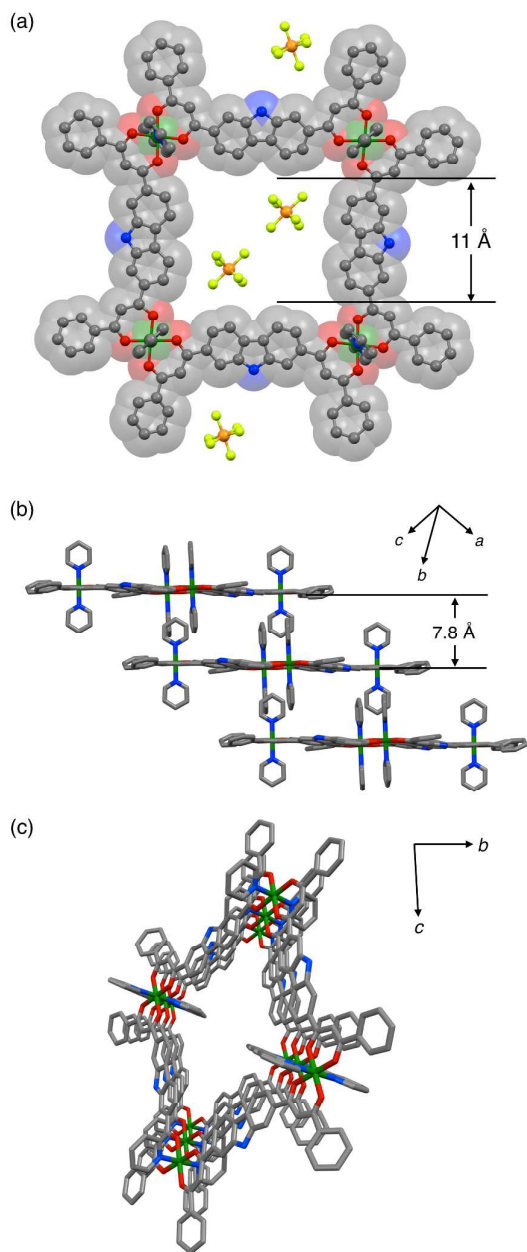
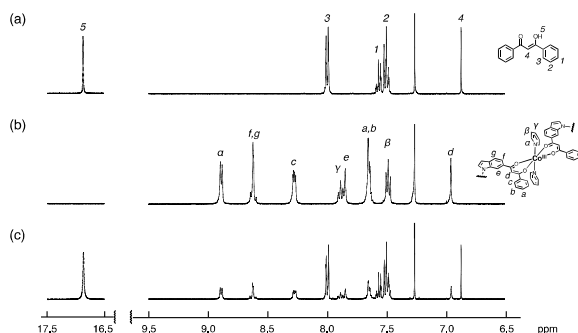


Figure 6. (a) Top view of the X-ray crystal structure of the L^2 :Co(III) ion = 4:4 macrocycle $[Co(III)_4L_4(py)_8] \cdot 4PF_6$. (b) Side view and (c) view along the a -axis of three $[Co(III)_4L_4(py)_8]$ moieties. The hydrogen atoms and alkyl side chains of the macrocycle, and crystal solvents have been removed for clarity. Color code: Co, green; C, gray; N, blue; O, red; P, orange; F, yellow.



This journal is © The Royal Society of Chemistry 20xx

Figure 7. Aromatic region of the 1H -NMR spectra of (a) 1,3-diphenylpropane-1,3-dione, (b) $[Co(III)_4L_4(py)_8] \cdot 4PF_6$, and (c) a mixture of 1,3-diphenylpropane-1,3-dione (10 mM) and $[Co(III)_4L_4(py)_8] \cdot 4PF_6$ (1 mM) after the incubation in $CDCl_3$ at 20 °C for 15 d.

To evaluate the kinetic stability of the macrocycle $[Co(III)_4L_4(py)_8] \cdot 4PF_6$, the 1H -NMR spectrum of $[Co(III)_4L_4(py)_8] \cdot 4PF_6$ was recorded in pyridine- d_5 . If the exchange of the axial pyridine actually occurs in the presence of an excess amount of pyridine- d_5 , it is expected to decrease the size of the signals corresponding to the axial nondeuterated pyridines of $[Co(III)_4L_4(py)_8] \cdot 4PF_6$ as a function of time. However, no decrease in the signals was observed after standing the solution at room temperature for 20 d (Figure S5). As in the case of pyridine- d_5 , the 1H -NMR spectra of $[Co(III)_4L_4(py)_8] \cdot 4PF_6$ did not change in other solvents such as CH_3CN-d_3 and $DMSO-d_6$. Furthermore, no ligand exchange on $[Co(III)_4L_4(py)_8] \cdot 4PF_6$ was observed after the coexistence with an excess amount of 1,3-diphenylpropane-1,3-dione in $CDCl_3$ at 20 °C at least within 15 d as shown in Figure 7. Thus, the discrete macrocyclic structure generated via metal-mediated self-assembly successfully afforded kinetically stable $[Co(III)_4L_4(py)_8] \cdot 4PF_6$ by the oxidation of the Co(II) centers to inert Co(III).

Experimental

General Information

The synthetic procedures were carried out under anhydrous nitrogen atmosphere, unless otherwise specified. All the reagents and solvents were purchased at the highest commercial quality available and used as received without further purification, unless otherwise stated. 2,7-Diacetyl-9H-carbazole **1** was synthesized according to a previous report.^[13] The 1H , and ^{13}C spectra were recorded using a JEOL JNM-ECS400 (400 MHz for 1H ; 100 MHz for ^{13}C) spectrometer, and JEOL JNM-A600 (600 MHz for 1H ; 150 MHz for ^{13}C) spectrometer at a constant temperature of 298 K. Tetramethylsilane (TMS) was used as the internal standard for the 1H and ^{13}C NMR measurements in $CDCl_3$. The elemental analyses were performed using a Yanaco MT-6 analyzer. The silica gel column chromatographies and thin-layer chromatography (TLC) were performed using Merck silica gel 60 and Merck silica gel 60 (F254) TLC plates, respectively. The ESI mass spectrometry was performed using a Waters LCT-Premier XE spectrometer, controlled using the Masslynx software, or a Bruker Daltonics micrOTOF-Q II spectrometer, controlled using the Compass software. The MALDI-TOF mass spectrometry was performed using a Bruker Daltonics Ultraflex III spectrometer.

The absorption spectra were recorded using a Hitachi U-4100 spectrophotometer in $CHCl_3$ solutions at 20 ± 0.1 °C in 1.0-cm quartz cells.

Single-Crystal X-ray Structural Analysis

The synchrotron X-ray diffraction analysis for $[\text{Co}(\text{III})_4\text{L}_4(\text{py})_8]\cdot 4\text{PF}_6$ was carried out at the BL02B1 beam-line in SPring-8 with the approval of the Japan Synchrotron Radiation Research Institute (JASRI) using an X-ray diffractometer equipped with a Rigaku Mercury2CCD detector ($\lambda = 0.6890 \text{ \AA}$). A data set was obtained by merging two data sets measured with 1.0° oscillation ($\omega = 0\text{--}180^\circ$) for 16.0 s radiation with 69.7-mm detector distance, $\phi = 0$ and 180° , $\chi = 45^\circ$, and $2\theta = -25^\circ$. The collected X-ray diffraction data were processed using the *RAPID AUTO* software. The structure was solved by Sir92 and refined by full-matrix least-squares on F^2 using the SHELX2014¹⁸ and *Yadokari-XG* software.¹⁹ The crystals diffracted very weakly due to the flipping of flexible alkyl chain moieties and the presence of a large amount of disordered solvent molecules in the inside and outside of the crystal void. The geometrical restraints, i.e., DFIX, DELU, SAME, SIMU, and ISOR, especially on the alkyl side chains and PF_6 unit, were used in the refinements. The detailed crystal data and structure refinement for $[\text{Co}(\text{III})_4\text{L}_4(\text{py})_8]\cdot 4\text{PF}_6$ are shown in Supporting Information.

Preparation of 2. A mixture of 2,7-diacetyl-9H-carbazole **1** (1.5 g, 6.0 mmol) and K_2CO_3 (2.5 g, 18 mmol) was stirred in DMF (15 mL) at 70°C for 1 h. Then, *tert*-butyl bromoacetate (1.8 mL, 12 mmol) was added to the suspension. The resulting mixture was stirred at 70°C for another 5 h. The reaction mixture was poured into H_2O (300 mL), and the resulting precipitate was collected by filtration. The crude pale brown solid was purified by recrystallization from MeCN (100 mL), affording compound **2** as a pale brown solid (2.0 g, 92% yield). ^1H NMR (400 MHz, CDCl_3/TMS): δ ppm 8.19 (dd, $J = 1.9$ Hz, 8.1 Hz, 2H), 8.03 (d, $J = 0.7$ Hz, 2H), 7.90 (dd, $J = 1.5$ Hz, 8.1 Hz, 2H), 5.04 (s, 2H), 2.74 (s, 6H), 1.45 (s, 9H). ^{13}C NMR (150 MHz, CDCl_3/TMS): δ ppm 198.1, 166.9, 141.9, 135.9, 126.1, 121.2, 120.6, 108.9, 83.3, 45.4, 28.0, 27.1. ESI-TOF-MS (positive) $m/z = 388.1$ $[\text{M} + \text{Na}]^+$. 388.2 calcd for $[\text{M} + \text{Na}]^+$.

Preparation of compound 3. A 1M LDA solution (20 mL, 20 mmol) was added to a solution of compound **2** (2.0 g, 5.5 mmol) in THF (400 mL) at -40°C . The solution was stirred for 15 min. Then, benzoyl cyanide (1.6 mL, 13.2 mmol) in THF (100 mL) was added dropwise to the mixture. The resulting mixture was stirred at -40°C for 18 h. H_2O (100 mL) and 10% aqueous NaH_2PO_4 (200 mL) were added to the reaction mixture to quench the reaction. The separated organic phase was washed with 10% aqueous NaH_2PO_4 (100 mL \times 4) and brine (100 mL \times 3), dried over anhydrous Na_2SO_4 , filtered, and evaporated, affording a yellow solid. The crude compound was purified by reprecipitation from a mixture of CH_2Cl_2 (300 mL) and MeOH (600 mL), followed by recrystallization from pyridine, affording compound **3** as a yellow solid. The filtrate was preadsorbed onto silica gel (20 g) and purified by silica gel column chromatography ($4.5\phi \times 14$ cm, CH_2Cl_2), affording compound **3**. In total, compound **3** (1.4 g) was obtained in 44% yield. ^1H NMR (400 MHz, CDCl_3/TMS): δ ppm 17.05 (s, 2H), 8.21 (d, $J = 8.2$ Hz, 2H), 8.10 (s, 2H), 8.04 (d, $J = 7.6$ Hz, 2H), 7.60–7.50 (m, 6H), 7.01 (s, 2H), 5.09 (s, 2H), 1.47 (s, 9H). ^{13}C NMR (150 MHz,

CDCl_3/TMS): δ ppm 186.0, 185.5, 166.9, 141.9, 135.6, 134.3, 132.5, 128.7, 127.2, 125.9, 121.1, 119.1, 108.2, 93.6, 83.3, 45.6, 28.0. ESI-TOF-MS (positive) $m/z = 596.1$ $[\text{M} + \text{Na}]^+$. 596.2 calcd for $[\text{M} + \text{Na}]^+$.

Preparation of compound 4. Compound **3** (1.66 g, 2.9 mmol) was dissolved in a mixture of TFA (25 mL) and CH_2Cl_2 (60 mL). The solution was stirred for 5.5 h at room temperature. After Et_2O (150 mL) was added to the reaction mixture, the resulting precipitate was collected by filtration and dried under reduced pressure, affording **4** as a yellow solid (1.45 g, 97% yield). ^1H NMR (400 MHz, $\text{DMSO}-d_6/\text{TMS}$): δ ppm 17.42 (br, 2H), 8.48–8.46 (m, 4H), 8.22 (d, $J = 7.6$ Hz, 4H), 8.12 (d, $J = 8.4$ Hz, 2H), 7.69 (t, $J = 7.2$ Hz, 3H), 7.26 (t, $J = 7.4$ Hz, 4H), 7.54 (s, 2H), 5.59 (s, 2H). ^{13}C NMR (150 MHz, $\text{DMSO}-d_6/\text{TMS}$): δ ppm 185.8, 184.7, 170.0, 141.6, 134.6, 133.1, 132.9, 128.8, 127.3, 125.2, 121.4, 118.8, 109.2, 93.5. ESI-TOF-MS (positive) $m/z = 540.1$ $[\text{M} + \text{Na}]^+$. 540.1 calcd for $[\text{M} + \text{Na}]^+$.

Synthesis of H₂L. Compound **4** (5.1 g, 9.8 mmol), 1-[bis(dimethylamino)methylene]-1H-1,2,3-triazolo[4,5-b]pyridinium 3-oxid hexafluorophosphate (HATU) (4.4 g, 11.7 mmol), and 2,4,6-trimethylpyridine (TMP) (2.6 mL, 19.7 mmol) were dissolved in NMP (100 mL), and the solution was stirred for 15 min. Diocetylamine (3.2 mL, 10.6 mmol) was added, and the resulting mixture was stirred for 3.5 h at 80°C . A solution of 1 M aqueous HCl (150 mL) was added to the reaction mixture. The resulting yellow precipitate was collected by filtration, washed with H_2O (50 mL \times 3) and MeCN (30 mL \times 4) successively, and dried under reduced pressure, affording a yellow solid (7.0 g). The crude product was purified by recrystallization from pyridine (80 mL), affording **H₂L** as a yellow solid (6.4 g, 90% yield). ^1H NMR (400 MHz, CDCl_3/TMS): δ ppm 17.05 (s, 2H), 8.20 (d, $J = 8.6$ Hz, 2H), 8.07 (s, 2H), 8.03 (d, $J = 7.0$ Hz, 4H), 7.87 (dd, $J = 1.2$, 8.5 Hz, 2H), 7.60–7.56 (m, 2H), 7.53–7.49 (m, 4H), 6.99 (s, 2H), 5.24 (s, 2H), 3.43 (t, $J = 7.9$ Hz, 2H), 3.36 (t, $J = 7.8$ Hz, 2H), 1.67 (br, 2H), 1.55–1.52 (m, 10H, including H_2O), 1.34–1.18 (m, 21H), 0.89 (t, $J = 7.2$ Hz, 3H), 0.81 (t, $J = 7.0$ Hz, 3H). ^{13}C NMR (150 MHz, CDCl_3/TMS): δ ppm 186.0, 185.3, 165.7, 142.1, 135.7, 134.2, 132.4, 128.7, 127.2, 125.9, 121.0, 118.9, 108.3, 93.6, 47.8, 46.8, 45.0, 31.79, 31.76, 29.4, 29.3, 29.25, 29.22, 27.7, 27.1, 27.0, 22.64, 22.59, 14.1, 14.0. ESI-TOF-MS (positive) $m/z = 763.3$ $[\text{M} + \text{Na}]^+$. 763.4 calcd for $[\text{M} + \text{Na}]^+$. Elemental Anal. calcd for $\text{C}_{48}\text{H}_{56}\text{N}_2\text{O}_5$ (M): C, 77.81; H, 7.62; N, 3.78. Found. C, 77.93; H, 7.60; N, 3.80 (0.12% error).

Preparation of $[\text{Co}(\text{III})_4\text{L}_4(\text{py})_8]\cdot 4\text{PF}_6$. A solution of $\text{Co}(\text{OAc})_2\cdot 4\text{H}_2\text{O}$ (52 mg, 207 μmol) in a mixture of pyridine (1.0 mL) and CHCl_3 (9.0 mL) was added to a solution of **H₂L** (148 mg, 199 μmol) and DBU (60 μL , 404 μmol) in CHCl_3 (190 mL). The resulting solution was stirred for 5 h at room temperature, and then cooled to -40°C . A solution of chloranil (155 mg, 632 μmol) in CHCl_3 (50 mL) was added dropwise to the reaction mixture for 20 min, and the resulting mixture was stirred for another 10 min at -40°C . The reaction mixture was evaporated, and the residue was sonicated in MeOH (20 mL). The insoluble substances in MeOH were removed by filtration. Then, NH_4PF_6 (1.4 g, 8.6 mmol) in MeOH (20 mL) were added to the filtrate, and the obtained precipitate was filtered and washed with H_2O

(15 mL × 2), affording a dark brown solid (221 mg). The crude compound was purified by silica gel column chromatography (3.5φ × 15 cm, CH₂Cl₂/MeOH = 1:0–49:1), affording a dark red solid. This compound was further purified by reprecipitation from CH₂Cl₂ and toluene twice, affording the titled compound as a reddish brown solid (95 mg, 43% yield). ¹H NMR (400 MHz, CDCl₃/TMS): δ ppm 8.87 (d, *J* = 5.6 Hz, 4H), 8.64–8.60 (m, 4H), 8.28–8.26 (m, 4H), 7.88 (t, *J* = 7.7 Hz, 2H), 7.84 (s, 2H), 7.65–7.64 (m, 6H), 7.48 (dd, *J* = 7.1, 7.1 Hz, 4H), 6.96 (s, 2H), 5.47 (s, 2H), 3.57 (br, 2H), 3.19 (br, 2H), 1.67 (br, 2H), 1.42 (br, 4H), 1.13–1.06 (m, 19H), 0.81–0.75 (m, 6H). ESI-TOF-MS (positive) *m/z* = 955.9 [M – 4PF₆]⁴⁺, 955.9 calcd [M – 4PF₆]⁴⁺. Elemental Anal. calcd for C₂₃₂H₂₅₆N₁₆O₂₀Co₄P₄F₂₄ (M): C, 63.27; H, 5.86; N, 5.09. Found. C, 63.57; H, 5.87; N, 5.06 (0.30% error).

Conclusions

Self-assembly via reversible metal complexation is an efficient method to synthesize large molecular architectures from small components in solutions. However, the ligand exchange reactions with coexistent substances and disassembly in highly diluted solutions are inherent in molecular architectures. In this study, we demonstrated the locking of the structure of a macrocycle, synthesized by metal-coordination-based self-assembly, via the oxidation of the central metal ions. This strategy is very effective to save the molecular architecture from kinetic instability caused by reversible bond formation. Further, it can be used as a general method for the construction of larger and more complex molecular architectures because of its simplicity. The synthesized macrocycle was robust and stable even in the presence of excess competitive ligands, and the size of the inner cavity was sufficiently large to accommodate small guest molecules. Hence, the investigation on the size- and/or site-selective molecular recognition in the inner cavity of the macrocycle is underway. Further, the strategy will be used to synthesize more complex molecular architectures via multistage and alternate self-assembly and oxidation, utilizing the stability of the linkage.

Acknowledgements

This work was supported by a JSPS KAKENHI Grant-in-Aid for Scientific Research (A) (Number 15H02167) to KT and a JSPS KAKENHI Grant-in-Aid for Young Scientists (B) (Number 21750060) to YY. The single-crystal synchrotron radiation X-ray diffraction measurements were carried out at the BL02B1/Spring-8 and BL38B1/Spring-8 in Japan (Proposal Nos. 2103B1422 and 2014B1175).

Notes and references

- (a) B. J. Holliday, C. A. Mirkin, *Angew. Chem. Int. Ed.* 2001, **40**, 2022–2043; (b) G. F. Swiegers, T. J. Malefetse, *Chem. Rev.* 2000, **100**, 3483–3537.
- (a) M. Fujita, D. Oguro, M. Miyazawa, H. Oka, K. Yamaguchi, K. Ogura, *Nature*, 1995, **378**, 469–471; (b) D. L. Caulder, R. E. Powers, T. N. Parac, K. N. Raymond, *Angew. Chem. Int. Ed.*

- 1998, **37**, 1840–1843; (c) B. Olenyuk, J. A. Whiteford, A. Fechtenkötter, P. J. Stang, *Nature*, 1999, **398**, 796–799; (d) R. Chakrabarty, P. S. Mukherjee, P. J. Stang, *Chem. Rev.* 2011, **111**, 6810–6918.
- (a) M. Aoyagi, K. Biradha, M. Fujita, *J. Am. Chem. Soc.* 1999, **121**, 7457–7458; (b) S. Tashiro, M. Tominaga, T. Kusukawa, M. Kawano, S. Sakamoto, K. Yamaguchi, M. Fujita, *Angew. Chem. Int. Ed.* 2003, **42**, 3267–3270; (c) T. Yamaguchi, S. Tashiro, M. Tominaga, M. Kawano, T. Ozeki, M. Fujita, *J. Am. Chem. Soc.* 2004, **126**, 10818–10819; (d) W. Meng, J. K. Clegg, J. R. Nitschke, *Angew. Chem. Int. Ed.* 2012, **51**, 1881–1884.
- (a) M. Fujita, J. Yazaki, K. Ogura, *J. Am. Chem. Soc.* 1990, **112**, 5645–5647; (b) G. R. Newkome, T. J. Cho, N. Moorefield, G. R. Baker, R. Cush, P. S. Russo, *Angew. Chem. Int. Ed.* 1999, **38**, 3717–3721; (c) S. Leininger, B. Olenyuk, P. J. Stang, *Chem. Rev.* 2000, **100**, 853–908; (d) S.-H. Hwang, P. Wang, C. N. Moorefield, L. A. Godínez, J. Manríquez, E. Bustos, G. R. Newkome, *Chem. Commun.* 2005, 4672–4674; (e) J. K. Clegg, L. F. Lindoy, B. Moubaraki, K. S. Murray, J. C. McMurtrie, *Dalton Trans.* 2004, 2417–2423.
- Q.-F. Sun, J. Iwasa, D. Ogawa, Y. Ishido, S. Sato, T. Ozeki, Y. Sei, K. Yamaguchi, M. Fujita, *Science*, 2010, **328**, 1144–1147.
- D. Fujita, A. Takahashi, S. Sato, M. Fujita, *J. Am. Chem. Soc.* 2011, **133**, 13317–13319.
- M. Weck, B. Mohr, J.-P. Sauvage, R. H. Grubbs, *J. Org. Chem.* 1999, **64**, 5463–5471.
- D. A. Leigh, R. G. Pritchard, A. J. Stephens, *Nature Chem.* 2014, **6**, 978–982.
- S. J. Lippard, J. M. Berg, *Principles of Bioinorganic Chemistry*, University Science Books, California, 1994, pp. 28–29.
- (a) L. J. Charbonniere, G. Bernardinelli, C. Piguet, A. M. Sargeson, A. F. Williams, *J. Chem. Soc., Chem. Commun.* 1994, 1419–1420; (b) S. Rigault, C. Piguet, G. Bernardinelli, G. Hopfgartner, *Angew. Chem. Int. Ed.* 1998, **37**, 169–172; (c) S. Rigault, C. Piguet, *J. Am. Chem. Soc.* 2000, **122**, 9304–9305; (d) S. Rigault, C. Piguet, G. Bernardinelli, G. Hopfgartner, *J. Chem. Soc., Dalton Trans.* 2000, 4587–4600.
- (a) M. Cantuel, G. Bernardinelli, G. Müller, J. P. Riehl, C. Piguet, *Inorg. Chem.* 2004, **43**, 1840–1849; (b) M. Cantuel, G. Bernardinelli, D. Imbert, J.-C. G. Bünzli, G. Hopfgartner, C. Piguet, *J. Chem. Soc., Dalton Trans.* 2002, 1929–1940; (c) S. G. Telfer, N. Tajima, R. Kuroda, M. Cantuel, C. Piguet, *Inorg. Chem.* 2004, **43**, 5302–5310; (d) S. Torelli, D. Imbert, M. Cantuel, G. Bernardinelli, S. Delahaye, A. Hauser, J.-C. G. Bünzli, C. Piguet, *Chem. Eur. J.* 2005, **11**, 3228–3242; (e) M. Cantuel, F. Gummy, J.-C. G. Bünzli, C. Piguet, *Dalton Trans.* 2006, 2647–2660; (f) G. Canard, C. Piguet, *Inorg. Chem.* 2007, **46**, 3511–3522; (g) L. Aboshyan–Sorgho, C. Besnard, P. Pattison, K. R. Kittilstved, A. Aebischer, J.-C. G. Bünzli, A. Hauser, C. Piguet, *Angew. Chem. Int. Ed.* 2011, **50**, 4108–4112.
- P. R. Symmers, M. J. Burke, D. P. August, P. I. T. Thomson, G. S. Nichol, M. R. Warren, C. J. Campbell, P. J. Lusby, *Chem. Sci.* 2015, **6**, 756–760.
- P. He, H. H. Wang, J. X. Shi, G. Wang, M. L. Gong, *Inorg. Chem.* 2009, **48**, 11382–11387.
- N. Tian, D. Lenkeit, S. Pelz, L. H. Fischer, D. Escudero, R. Schiewek, D. Klink, O. J. Schmitz, L. González, M. Schäferling, E. Holder, *Eur. J. Org. Chem.* 2010, **30**, 4875–4885.
- S. Wiles, P. Watts, S. J. Haswell, E. P.-Villar, *Tetrahedron Lett.* 2002, **43**, 2945–2948.
- J. L. Ault, H. J. Harries, *Inorg. Chim. Acta* 1977, **25**, 65–69.
- The direct synthesis of [Co(III)₄L₄(py)₈]⁴⁺ from Co(III)(acetylacetonate)₃ with H₂L was not proceeded at the similar condition.
- G. M. Sheldrick, *Acta Cryst.* 2008, **A64**, 112–122.

ARTICLE

Journal Name

- 19 Yadokari-XG, Software for Crystal Structure Analyses, K. Wakita, 2001; Release of Software (Yadokari-XG 2009) for Crystal Structure Analyses, C. Kabuto, S. Akine, T. Nemoto, and E. Kwon, *J. Cryst. Soc. Jpn.* 2009, **51**, 218–224.